composition of C_4F_9I on diamond(100) are shown in Fig. 4. Here the initial desorption of C_4F_9I upon heating from 119 to 300 K can be seen from the behavior of the F(1*s*), I(3*d*), and diamond C(1*s*) features. The first stage of the decrease in F(1*s*) integrated intensity, due to the loss of chemically bound fluorine, occurred slowly in the temperature range from 300 to 900 K as C_4F_9– species thermally decomposed to produce C–F bonds on the diamond surface (compare with Figs. 2 and 3). The second stage of F(1*s*) depletion was observed at temperatures above about 900 K as surface-bound fluorine was removed. The stability of the chemisorbed diamond surface C–F bonds produced from anchored C_4F_9– species was similar or superior to the behavior for similar C–F– groups produced by direct fluorination with F atoms (6).

The coverage of fluorine on diamond(100) has been estimated using C(1*s*) and F(1*s*) intensities from clean and fluorinated diamond, respectively (*11*). An electron mean free path of $\lambda = 14$ Å (*16*) for C(1*s*) electrons and XPS relative sensitivity factors of $S_C = 0.2$ and $S_F = 1.0$ (*17*) were used. For the anchored C_4F_9– layer produced by heating to 300 K after x-ray irradiation of the C_4F_9I layer, N_F/N_C was equal to 2.0, where N_C is the number of surface C atoms on the clean diamond surface, and N_F is the number of surface F atoms in the anchored C_4F_9– species. When the C_4F_9– species were decomposed almost completely near 700 K, N_F/N_C equaled 0.6 for a single experiment. Similar experiments with CF_3I only yielded N_F/N_C of ~0.2 at 300 K. Thus, the use of a longer chain perfluoroalkyl iodide drives the fluorination of diamond surfaces to higher levels.

The experiments described above were carried out on atomically clean diamond surfaces to study the inherent reactivity of the diamond surface. However, diamond surfaces are passivated by the presence of surface C–H bonds (9), and this passivation would be expected to make the method described above impractical in most technological cases because of the need for high-temperature treatment of the passivated diamond to remove surface hydrogen before fluorination. We repeated the fluorination experiments on a deuterium-passivated diamond(100) surface and found evidence for the production of DI species at 119 K and for the subsequent fluorination of the diamond(100) surface (*11*). Apparently, the free radical species produced by radiation-induced decomposition of the C–I bond in C_4F_9I molecules are able to abstract D atoms from C–D bonds on the diamond surface to form DI and to facilitate attachment of C_4F_9– groups to the diamond surface (*11*). This observation indicates that the radiation-induced fluorination of hydrogen-terminated diamond surfaces that are technologically useful can be achieved by the methods described above.

The radiation-induced mechanism for the fluorination of diamond was not investigated in this work. A variety of radiation-induced processes could be responsible, including direct photoionization by x-rays and electron-stimulated dissociation (*18*) due to secondary electron emission from the irradiated substrate. Stray electrons produced in the x-ray source are not responsible for this effect (*11*). It is well known that the weak C–I bond in C_4F_9I (bond energy = 2.05 eV) (*3*, *12*) can be easily photolyzed, and this route is commonly used to induce free radical chemistry in homogeneous phase (*19*). In the stages of fluorination and decomposition of fluorinated diamond surfaces (Fig. 5), C–I bond scission at 120 K, followed by radical attachment to the diamond surface, precedes the thermal decomposition of anchored C_4F_9– groups to yield F atoms that are chemically bonded to the diamond surface.

REFERENCES AND NOTES

1. P. K. Bachmann and R. Messier, *Chem. Eng. News* **67** (no. 20), 24 (15 May 1989); J. E. Field, *The Properties of Diamonds* (Academic Press, New York, 1979); *The Properties of Natural and Synthetic Diamonds* (Academic Press, New York, 1992); R. Pool, *Science* **249**, 27 (1990); B. J. Feder, *New York Times*, 21 February 1990, p. C4; D. E. Koshland Jr., *Science* **250**, 1637 (1990).
2. S. K. Ritter, *Chem. Eng. News* **73** (no. 9), 39 (27 February 1995); K. E. Spear, *J. Am. Ceram. Soc.* **72**, 171 (1989).
3. R. Weast, Ed., *Handbook of Chemistry and Physics* (CRC Press, Boca Raton, FL, ed. 63, 1982), p. F-199.
4. D. S. Y. Hsu and N. H. Turner, paper presented at Fourth SDIO/First Office of Naval Research Diamond Technology Initiative Symposium, Arlington, VA, 11 to 13 July 1989.
5. D. E. Patterson, R. H. Hauge, J. L. Margrave, *Mater. Res. Soc. Symp. Proc.* **140**, 351 (1989).
6. A. Freedman and C. D. Stinespring, *Appl. Phys. Lett.* **57**, 1194 (1990); *Mater. Res. Soc. Symp. Proc.* **204**, 571 (1991); *Proc. Electrochem. Soc.* **91**, 494 (1991); *New Diamond Sci. Technol. Proc. Int. Conf.* **2**, 321 (1991).
7. J. F. Morar *et al.*, *Phys. Rev. B* **33**, 1340 (1986); J. F. Morar *et al.*, *ibid.*, p. 1346.
8. P. Cadman, J. D. Scott, J. M. Thomas, *J. Chem. Soc. Chem. Commun.* **1975**, 654 (1975).
9. J. Wei, V. S. Smentkowski, J. T. Yates Jr., *Critical Reviews in Surface Chemistry* (CRC Press, Boca Raton, FL, in press).
10. A. Katz, S. P. Murarka, Y. I. Nissim, J. M. E. Harper, *Mater. Res. Soc. Symp. Proc.* **260**, 905 (1992).
11. V. S. Smentkowski, J. T. Yates Jr., X. Chen, W. A. Goddard III, in preparation.
12. E. N. Okafo and E. Whittle, *Int. J. Chem. Kinetics* **7**, 287 (1975).
13. V. S. Smentkowski and J. T. Yates Jr., *J. Vac. Sci. Technol. A* **11**, 3002 (1993).
14. V. S. Smentkowski, H. J. Jänsch, M. A. Henderson, J. T. Yates Jr., *Surf. Sci.* **330**, 207 (1995).
15. P. Cadman, J. D. Scott, J. M. Thomas, *Surf. Interface Anal.* **1**, 115 (1979).
16. B. B. Pate, *Surf. Sci.* **165**, 83 (1986); S. Evans, R. G. Pritchard, J. M. Thomas, *J. Phys. C.* **10**, 2483 (1977).
17. *Empirical Atomic Sensitivity Factors for MgKα Irradiation* (Leybold Vacuum Products, Cologne, Germany, 1984); C. D. Wagner, W. M. Riggs, L. E. Davis, J. F. Moulder, G. E. Muilenberg, *Handbook of X-Ray Photoelectron Spectroscopy* (Perkin-Elmer, Eden Prairie, MN, 1979).
18. R. D. Ramsier and J. T. Yates Jr., *Surf. Sci. Rep.* **12**, 243 (1991).
19. H. Okabe, *Photochemistry of Small Molecules* (Wiley, New York, 1978).

20. We thank the Air Force Office of Scientific Research for support of this work (contract F49620-92-J-0192).

27 June 1995; accepted 23 October 1995

Functional Evidence for Indirect Recognition of G·U in $tRNA^{Ala}$ by Alanyl-tRNA Synthetase

K. Gabriel, Jay Schneider, William H. McClain*

The structural features of the G·U wobble pair in *Escherichia coli* alanine transfer RNA ($tRNA^{Ala}$) that are associated with aminoacylation by alanyl-tRNA synthetase (AlaRS) were investigated in vivo for wild-type $tRNA^{Ala}$ and mutant tRNAs with G·U substitutions. $tRNA^{Ala}$ with G·U, C·A, or G·A gave similar amounts of charged $tRNA^{Ala}$ and supported viability of *E. coli* lacking chromosomal $tRNA^{Ala}$ genes. $tRNA^{Ala}$ with G·C was inactive. Recognition of G·U by AlaRS thus requires more than the functional groups on G·U in a regular helix and may involve detection of a helical distortion.

RNA-protein interactions require the stable merging of two complementary tertiary structures. The G·U wobble base pair at positions 3 and 70 (3·10) of the acceptor helix in *E. coli* $tRNA^{Ala}$ is a major determinant of the interaction of this RNA with AlaRS during aminoacylation (*1*). The prevalent direct recognition hypothesis states that AlaRS interacts directly with functional groups of the G·U pair in the minor groove of an A-form helix (*2*). An alternative indirect recognition hypothesis states that AlaRS recognition of G·U in $tRNA^{Ala}$ depends on a local helical distortion promoted by G·U as well as on recognition of its functional groups (*3*). To distinguish between these hypotheses, we tested the in vivo aminoacylation capacity of

Department of Bacteriology, University of Wisconsin, Madison, WI 53706, USA.

*To whom correspondence should be addressed.

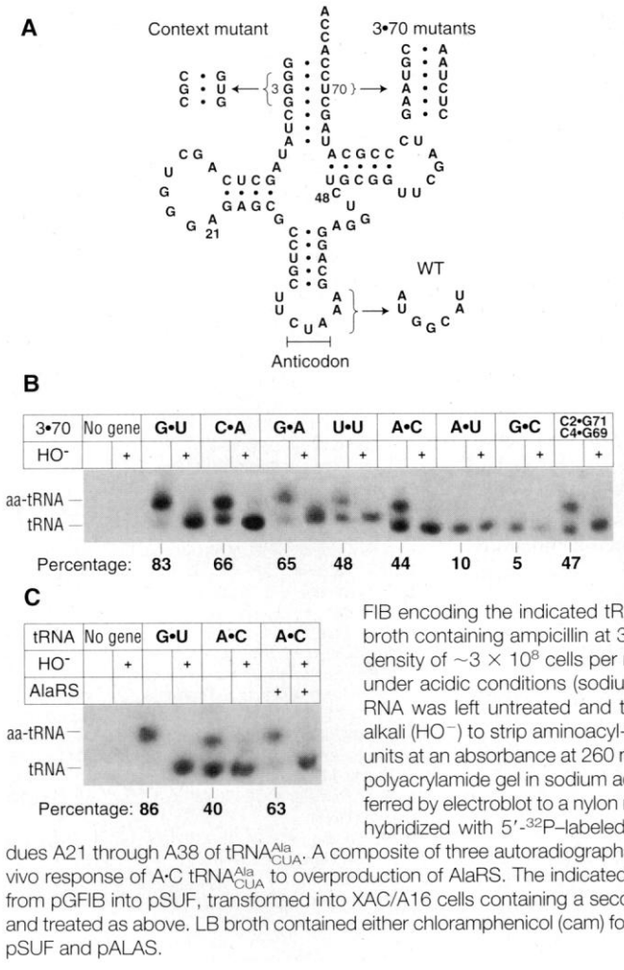

Fig. 1. (**A**) Diagram of $tRNA^{Ala}_{CUA}$ showing the mutants examined. Genes for $tRNA^{Ala}_{GGC}$ (WT) were constructed from the corresponding $tRNA^{Ala}_{CUA}$ genes in pGFIB (*3*, *11*). Genes that combined WT with particular 3·70 mutants are described in the text. (**B** and **C**) In vivo amounts of aminoacyl-tRNA (aa-tRNA) and uncharged tRNA in the $tRNA^{Ala}_{CUA}$ system. The calculated percentage of aminoacyl-tRNA [100 × (aminoacyl-tRNA)/(aminoacyl-tRNA + uncharged tRNA)] is shown (*12*). The percentage is considerably overestimated in weak G·C and A·U mutants because no correction was made for streaking of uncharged tRNA. In (B), *E. coli* XAC/A16 cells transformed with pGFIB encoding the indicated $tRNA^{Ala}_{CUA}$ gene were grown in LB broth containing ampicillin at 37°C. When the cells reached a density of ~3 × 10^8 cells per milliliter, total RNA was isolated under acidic conditions (sodium acetate, pH 5.2). Half of the RNA was left untreated and the other half was treated with alkali (HO^-) to strip aminoacyl-tRNAs. Samples (~0.5 μl, 0.05 units at an absorbance at 260 nm) were fractionated on a 6.5% polyacrylamide gel in sodium acetate (pH 5.2) buffer and transferred by electroblot to a nylon membrane. The membrane was hybridized with 5′-^{32}P–labeled probe complementary to residues A21 through A38 of $tRNA^{Ala}_{CUA}$. A composite of three autoradiographs is shown. In (C) is shown an in vivo response of A·C $tRNA^{Ala}_{CUA}$ to overproduction of AlaRS. The indicated $tRNA^{Ala}_{CUA}$ genes were recloned from pGFIB into pSUF, transformed into XAC/A16 cells containing a second AlaRS gene on pALAS (*13*), and treated as above. LB broth contained either chloramphenicol (cam) for pSUF or cam and ampicillin for pSUF and pALAS.

$tRNA^{Ala}$ with nucleotide substitutions that replace the G·U pair. With direct recognition, such substitutions would be expected to curtail aminoacylation, whereas with indirect recognition these substitutions would more likely be tolerated.

Genes for amber suppressor $tRNA^{Ala}$ ($tRNA^{Ala}_{CUA}$) were expressed from a plasmid so that transcription produced tRNA with a CUA amber anticodon in place of the wild-type UGC anticodon (*3*). The anticodon is not a major determinant of $tRNA^{Ala}$ aminoacylation. In vivo amounts of aminoacyl-tRNA and uncharged tRNA were determined by a quantitative Northern (RNA) blot analysis (*4*). The hybridization probe included the CUA anticodon and therefore bound $tRNA^{Ala}_{CUA}$ in preference to wild-type $tRNA^{Ala}$. Six 3·70 mutants of $tRNA^{Ala}_{CUA}$ with substitutions at the G·U pair and a context mutant with substitutions of the two base pairs that flank the G·U pair were examined (Fig. 1). Aminoacyl-tRNA and uncharged tRNA were evident in all cells except those expressing the A·U and G·C mutants, in which the amount of aminoacyl-tRNA was substantially reduced. The chemical identity of the amino acid in the aminoacyl-tRNA species was not directly determined. However, previous in vivo data allow us to conclude that Ala is the only amino acid esterified to $tRNA^{Ala}_{CUA}$ with G·U, C·A, G·A, U·U, and the context mutant changes and that Ala and some Lys are esterified to $tRNA^{Ala}_{CUA}$ with A·C (*3*).

Overproduction of AlaRS in cells in-

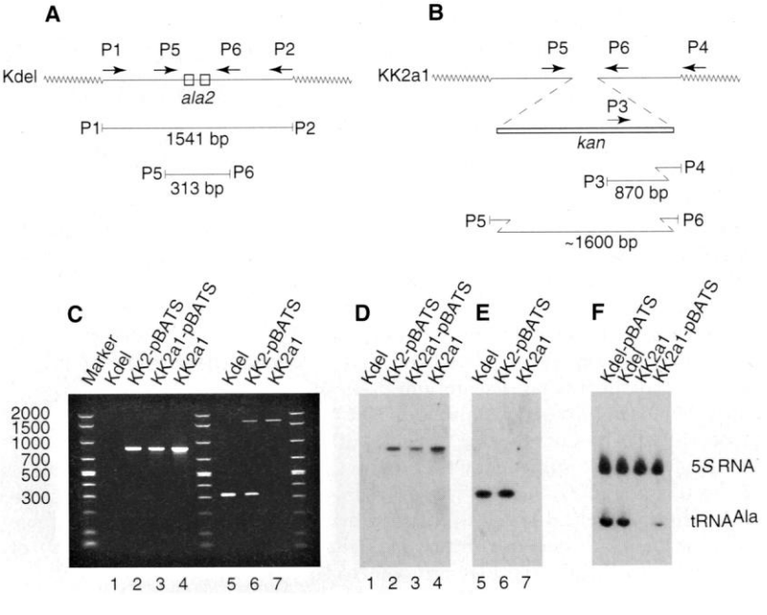

Fig. 2. Deletion of chromosomal *ala2* tRNA genes. (**A**) Ala2 chromosomal region in *E. coli* strain Kdel [*glyV55*Δ(*ArgF lac*), Δ(*tonB trpAB17*)/F′ *trpAUGA15*] showing priming sites and polymerase chain reaction (PCR) fragments (*14*). A 1541–base pair (bp) chromosomal fragment encompassing the two *ala2* genes was amplified from Kdel cells by PCR with primers P1 and P2 (*15*). The fragment was cloned into pGFIB, where the *ala2* genes were excised by restriction enzyme digestion and replaced by a kanamycin cassette. The modified fragment was then inserted into M13mp10::CAT (a nonreplicating vector that expresses its cam resistance only when integrated into a host chromosome) by restriction enzyme digestion and ligation. Strain Kdel carrying pBATS (a temperature-sensitive plasmid encoding $tRNA^{Ala}_{GGC}$) (*16*) was infected with M13mp10::CAT carrying the altered chromosomal sequence. The resulting partial diploid, strain KK2, was selected by cam and kanamycin resistance. (**B**) KK2 was induced with bile salts and screened for cam sensitivity and kanamycin (kan) resistance to detect a haploid mutant (KK2a1) with *ala2* genes replaced by kan^R. The excised M13 vector was lost by nonreplication. The *ala2* genes were nonessential, as the cells were viable after removal of pBATS. (**C**) PCR analysis with primers P3 and P4 generated the expected ~870-bp fragment in KK2 and KK2a1 but not in Kdel (lanes 1 to 4). Primers P5 and P6 generated the expected 313-bp fragment in Kdel, an ~1600-bp fragment in KK2a1, and both fragments in KK2 (lanes 5 to 7). Sizes are shown on the left in base pairs. (**D**) The ~870-bp fragment hybridized to primer P6, showing that the kan^R gene was inserted into the chromosome. (**E**) The 313-bp fragment hybridized to a probe complementary to positions 28 to 45 of Ala2 tRNA, demonstrating that the *ala2* genes were present in Kdel and KK2 but not in KK2a1. (**F**) Low molecular weight RNA was prepared from Kdel-pBATS, Kdel, KK2a1, and KK2a1-pBATS, fractionated by polyacrylamide gel electrophoresis, electroblotted, and hybridized (*11*) with a probe complementary to positions 34 to 53 of 5*S* RNA and with the Ala2 tRNA probe to confirm that KK2a1 does not make Ala2 tRNA. KK2a1 was modified by two P1 transductions to replace the *ala1* gene and most of the *rrnA* operon with a cam cassette and to introduce *relA1*, creating strain K45s1Δ*relA*.

creased by 58% the amount of aminoacyl-tRNA for A·C $tRNA^{Ala}_{CUA}$ (Fig. 1C), thus confirming the identification of aminoacyl-tRNA and uncharged tRNA species and the amount of aminoacylation of A·C $tRNA^{Ala}_{CUA}$ by AlaRS. The observation that C·A and G·A $tRNA^{Ala}_{CUA}$ were substantially aminoacylated (~80% of G·U $tRNA^{Ala}_{CUA}$), whereas G·C and A·U $tRNA^{Ala}_{CUA}$ were inactive, makes direct recognition unlikely. Previous in vitro aminoacylation of Ala minihelical RNAs by AlaRS identified functional groups on G·U that contribute to recognition (*2*), but further comparison with our results is complicated by systematic differences between in vivo and in vitro assays (*5*). Data obtained with the context mutant indicated that the base pairs flanking G·U in $tRNA^{Ala}$ also are important for aminoacylation (Fig. 1). These base pairs could be recognized directly by AlaRS or could contribute indirectly by influencing helix conformation.

If indirect recognition of G·U plays an important role in the interaction of $tRNA^{Ala}$ with AlaRS, then mutant tRNAs with C·A or G·A and a wild-type anticodon should be able to sustain global protein synthesis. To test this, we constructed an *E. coli* strain in which the chromosomal $tRNA^{Ala}$ genes were deleted (Fig. 2). We found that of the five $tRNA^{Ala}$ genes in *E. coli* (*6*), three (two *ala2* genes and one *ala1* gene) had to be deleted to produce lethality. The amount of Ala1 tRNA in the knockout strain (K45s1ΔA) was 65% of that in cells with three *ala1* genes (*7*); Ala2 tRNA was not detected (Fig. 2). K45s1ΔA cells grew well in rich Luria broth (LB) medium but slowly in minimal glucose medium, presumably because the increased biosynthetic demands were not met by available aminoacyl-$tRNA^{Ala}$. Growth was restored, however, when cells were transformed with a plasmid encoding wild-type $tRNA^{Ala}$ with a GGC anticodon ($tRNA^{Ala}_{GGC}$). K45s1ΔA cells transformed with a plasmid encoding $tRNA^{Ala}_{GGC}$ with G·C at 3·70 grew slower in LB medium than did the cells containing either the parent plasmid or a plasmid encoding $tRNA^{Ala}_{CUA}$ with G·C. This response suggested that uncharged G·C $tRNA^{Ala}_{GGC}$ was causing a stringent response (*8*) and retarding cell growth. We therefore introduced a *relA* allele into the knockout strains. The properties of strain K45s1Δ*ArelA* allowed a functional test of mutant $tRNA^{Ala}_{GGC}$.

The genes for wild-type and mutant $tRNA^{Ala}_{GGC}$ were introduced into K45s1Δ*ArelA* cells on a plasmid and LB liquid cultures prepared. The cultures were streaked on a split agar plate (Fig. 3). Of the five mutants tested, only the C·A and G·A mutants restored cell growth on minimal medium, indicating that these tRNAs were charged and functional. K45s1Δ*ArelA* cells expressing the other mutant tRNAs (U·U, A·C, and G·C) grew slowly, indicating that these tRNAs were not extensively charged. Introduction of a plasmid encoding $tRNA^{Ala}_{GGC}$ with G·U, but not the parent plasmid, restored growth of K45s1Δ*ArelA* cells (Fig. 3). A Northern (RNA) blot confirmed that $tRNA^{Ala}_{GGC}$ with G·U, C·A, or G·A was aminoacylated, whereas $tRNA^{Ala}_{GGC}$ with G·C was uncharged (*7*). The conversion of G·U to C·A or G·A in $tRNA^{Ala}_{GGC}$ thus preserves recognition by AlaRS.

The functional similarity of G·U, C·A, and G·A in $tRNA^{Ala}$ (Figs. 1 and 3), despite their structural differences, provides strong evidence that recognition of G·U by AlaRS depends on more than just the functional groups on G·U in the minor groove of an A-form helix. These structural differences include inversion of the purine-pyrimidine orientation and a purine-purine mismatch. Moreover, no functional group on G·U is spatially conserved in both C·A and G·A. However, G·U was superior to C·A and G·A in both functional tests of $tRNA^{Ala}$. Recognition of $tRNA^{Ala}$ by AlaRS may thus depend on two properties of the G·U pair: its functional groups and its ability to promote a local helical distortion. The functional groups on G·U could interact with AlaRS or help build the helical distortion, or both. A distorted helix, together with the divalent metal binding site defined by the G·U pair (*9*), may be generally important in RNA recognition. The nuclear magnetic resonance structure of the functionally important G·U pair at the cleavage site of the group I intron RNA reveals a local distortion from regular A-form features (*10*). Ultimately, three-dimensional structures and thermodynamic parameters will be required for a full understanding of the role of G·U in $tRNA^{Ala}$ aminoacylation.

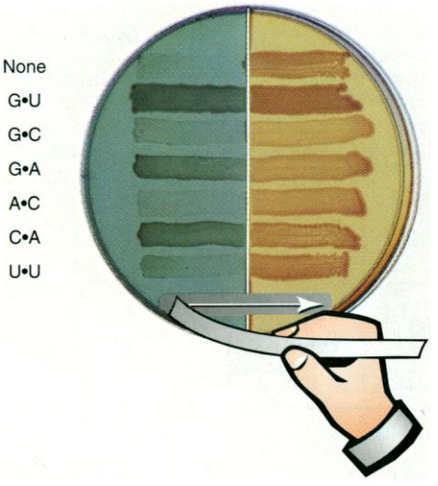

Fig. 3. Growth properties of K45s1Δ*ArelA* cells expressing mutant $tRNA^{Ala}_{GGC}$. A single colony of K45s1Δ*ArelA* transformed with pGFIB expressing the indicated mutant $tRNA^{Ala}_{GGC}$ was picked from an LB plate containing ampicillin, kanamycin, and cam, inoculated into LB broth containing ampicillin, kanamycin, and cam, and grown to a concentration of ~2×10^8 cells per milliliter at 33°C. A 2-μl sample of each culture was spotted onto minimal glucose, arginine, tryptophan, and ampicillin media on the left side of a split-agar plate. A sterile paper strip was immersed in the spot and streaked in a continuous pass from the minimal-medium side to the rich (LB + ampicillin) medium on the right side. The minimal medium contained bromthymol blue (~50 mg/liter) to increase the optical contrast between the agar and bacterial streaks. The plate was incubated at 33°C for 1.5 days.

REFERENCES AND NOTES

1. Y.-M. Hou and P. Schimmel, *Nature* **333**, 140 (1988); W. H. McClain and K. Foss, *Science* **240**, 793 (1988).
2. K. Musier-Forsyth *et al.*, *Science* **253**, 784 (1991).
3. W. H. McClain, Y.-M. Chen, K. Foss, J. Schneider, *ibid.* **242**, 1681 (1988).
4. U. Varshney, C.-P. Lee, U. L. RajBhandary, *J. Biol. Chem.* **266**, 24712 (1991); W. H. McClain, K. Gabriel, J. Schneider, *Nucleic Acids Res.* **22**, 522 (1994).
5. R. Giegé, J. D. Puglisi, C. Florentz, *Prog. Nucleic Acid Res. Mol. Biol.* **45**, 129 (1993).
6. Y. Komine, T. Adachi, H. Inokuchi, H. Ozeki, *J. Mol. Biol.* **212**, 579 (1990).
7. K. Gabriel, J. Schneider, W. H. McClain, unpublished data.
8. M. Cashel and K. E. Rudd, in *Escherichia coli and Salmonella typhimurium*, F. C. Neidhardt, Ed. (American Society for Microbiology, Washington, DC, 1987), vol. 2, pp. 1410–1438.
9. S. Limmer, H.-P. Hofmann, G. Ott, M. Sprinzl, *Proc. Natl. Acad. Sci. U.S.A.* **90**, 6199 (1993); F. H.-T. Allain and G. Varani, *Nucleic Acids Res.* **23**, 341 (1995).
10. F. H.-T. Allain and G. Varani, *J. Mol. Biol.* **250**, 333 (1995); J. A. Doudna, B. P. Cormack, J. W. Szostak, *Proc. Natl. Acad. Sci. U.S.A.* **86**, 7402 (1989); S. A. Strobel and T. R. Cech, *Science* **267**, 675 (1995).
11. W. H. McClain and K. Foss, *J. Mol. Biol.* **202**, 697 (1988).
12. Images of Northern blots were produced with a 445 SI Molecular Dynamics instrument and RNAs were quantified with ImageQuaNT software. Background correction was a rectangular area lacking discernible signal from the bottom of each sample lane. The percentages of aminoacyl-tRNA (Fig. 1) are single measurements except for the·3·70 mutants, for which the percentages are averages (SD ≤ 1.8%) of two gels on which the same RNA preparations were run.
13. Y. Komine, M. Kitabatake, T. Yokogawa, K. Nishikawa, H. Inokuchi, *Proc. Natl. Acad. Sci. U.S.A.* **91**, 9223 (1994).
14. P. Blum, D. Holzschu, H.-S. Kwan, D. Riggs, S. Artz, *J. Bacteriol.* **171**, 538 (1989); Y. V. Brun, R. Breton, P. Lanouette, J. Lapointe, *J. Mol. Biol.* **214**, 825 (1990); C. Condon, S. French, C. Squires, C. L. Squires, *EMBO J.* **12**, 4305 (1993); C. M. Hamilton, M. Aldea, B. K. Washburn, P. Babitzke, S. R. Kushner, *J. Bacteriol.* **171**, 4617 (1989).
15. The chromosome sequence was from the EcoSeq database, locus alaWecoM, accession number ES1002. The primer sequences used in Fig. 2 were as follows: P1, 5′-GGGAAATCAAAGAAGCTCCC-3′; P2, 5′-GGCACGACCGCCTTTCACGC-3′; P3, 5′-GTCAGCAACACCTTCTTCAC-3′; P4, 5′-CTTCAGCTTCCATCAACATT-3′; P5, 5′-AAGCGGCAAAAAGCAGAGAC-3′; and P6, 5′-GCAATTTGCCGTTGACACAT-3′.
16. pBATS is a low-copy plasmid constructed with a pSC101 temperature-sensitive replicon from pMAK705, an amp^R gene from pBR322, and a synthetic *ala2* gene from pGFIB.

17. We thank G. Björk, L. Kiessling, G. Varani, and M. Yarus for cogent discussions and S. Artz, H. Inokuchi, S. Kushner, J. Miller, and C. Squires for materials. Supported by U.S. Public Health Service grant GM42123.

21 September 1995; accepted 10 November 1995